HHS Public Access

Author manuscript

Mol Genet Metab. Author manuscript; available in PMC 2020 April 01.

Published in final edited form as:

Mol Genet Metab. 2019 April ; 126(4): 504–512. doi:10.1016/j.ymgme.2019.01.014.

Trps1 transcription factor regulates mineralization of dental tissues and proliferation of tooth organ cells

Morgan Goss[a,*], **Mairobys Socorro**[b,*], **Daisy Monier**[b], **Kostas Verdelis**[b], and **Dobrawa Napierala**[b]

[a]Institute of Oral Health Research, School of Dentistry, University of Alabama at Birmingham, Birmingham, AL, USA.

[b]Center for Craniofacial Regeneration, Dept. of Oral Biology, McGowan Institute for Regenerative Medicine, University of Pittsburgh School of Dental Medicine, Pittsburgh, PA, USA.

Abstract

Mutations of the *TRPS1* gene cause trichorhinophalangeal syndrome (TRPS), a skeletal dysplasia with dental abnormalities. TRPS dental phenotypes suggest that *TRPS1* regulates multiple aspects of odontogenesis, including the tooth number and size. Previous studies delineating *Trps1* expression throughout embryonic tooth development in mice detected strong *Trps1* expression in dental mesenchyme, preodontoblasts, and dental follicles, suggesting that TRPS dental phenotypes result from abnormalities in early developmental processes. In this study, $Trps1^{+/-}$ and $Trps1^{-/-}$ mice were analyzed to determine consequences of *Trps1* deficiency on odontogenesis. We focused on the aspects of tooth formation that are disturbed in TRPS and on potential molecular abnormalities underlying TRPS dental phenotypes. Microcomputed tomography analyses of molars were used to determine tooth size, crown shape, and mineralization of dental tissues. These analyses uncovered that disruption of one *Trps1* allele is sufficient to impair mineralization of dentin in both male and female mice. Enamel mineral density was decreased only in males, while mineralization of the root dental tissues was decreased only in females. In addition, significantly smaller teeth were detected in $Trps1^{+/-}$ females. Histomorphometric analyses of tooth organs showed reduced anterior-posterior diameter in $Trps1^{-/-}$ mice. BrdU-incorporation assay detected reduced proliferation of mesenchymal and epithelial cells in $Trps1^{-/-}$ tooth organs. Immunohistochemistry for Runx2 and Osx osteogenic transcription factors revealed changes in their spatial distribution in $Trps1^{-/-}$ tooth organs and uncovered cell-type specific requirements of *Trps1* for Osx expression. In conclusion, this study has demonstrated that *Trps1* is a positive regulator of cell proliferation in both dental mesenchyme and epithelium, suggesting that the microdontia in TRPS is likely due to decreased cell proliferation in developing tooth organs. Furthermore, the reduced mineralization observed in $Trps1^{+/-}$ mice may provide some explanation for the extensive dental caries reported in TRPS patients.

Author for Correspondence: Dobrawa Napierala, Ph.D., University of Pittsburgh, Department of Oral Biology, School of Dental Medicine, don11@pitt.edu.

*These authors equally contributed to this study.

Keywords

trichorhinophalangeal syndrome; transcription factor; tooth development; mineralization; cell proliferation

1. Introduction

TRPS1 is a zinc-finger protein that belongs to GATA family of transcription factors [1,2] The name of this protein stands for the trichorhinophalangeal syndrome (TRPS), an autosomal dominant genetic disorder caused by mutations in the *TRPS1* gene [3,4] TRPS patients have characteristic craniofacial features, skeletal defects, and a number of dental abnormalities [3-6]. Although dental abnormalities are considered a characteristic feature of TRPS, not all individuals with TRPS present with dental phenotypes and there is a considerable variability of oral manifestations even within the same family [5,7-9] The most frequently reported dental abnormalities include microdontia, supernumerary teeth, delayed tooth eruption, malocclusion, and extensive dental caries [3,5-7,10-12].

The clinical presentation of TRPS indicates that TRPS1 regulates development of endochondral bones, teeth, and hair. Heterozygous *Trps1*$^{+/-}$ mice show general skeletal and hair abnormalities similar to TRPS patients [7,13-16]. Consistently with a gene dose effect, more severe defects in development of endochondral bones and hair are present in *Trps1*$^{-/-}$ mice [13-16]. However, these mice die at birth, hence the effect of *Trps1* deficiency on postnatal tooth formation, including development of mineralized tissues, cannot be assessed. Analyses of *Trps1*$^{-/-}$ embryos detected no difference in the number of tooth organs, demonstrating that, unlike in humans, *Trps1* deficiency in mice does not result in aberrant tooth number [7].

Detailed analyses of *Trps1* expression during embryonic tooth development detected a specific and dynamic expression pattern. *Trps1* is highly expressed in dental mesenchyme throughout all stages of tooth organ formation beginning from the dental placode formation [7]. During cytodifferentiation, *Trps1* expression becomes restricted to preodontoblasts and dental follicle. The onset of dentin formation coincides with the downregulation of *Trps1* in odontoblasts [7,17] This expression pattern suggests that *Trps1* is involved in the tooth organ formation and differentiation of cells producing mineralizing matrix. The importance of *Trps1* for odontoblast maturation has been further demonstrated in in vitro studies, showing *Trps1* requirement for expression of mineralization-supporting proteins and for the initiation of mineralization. Specifically, expression of major osteogenic transcription factors Runx2 and Osx/Sp7 was significantly decreased in *Trps1* deficient odontoblast cells [18].

Considering the results of these in vitro studies and the specific *Trps1* expression pattern during tooth development, we hypothesized that detailed analyses of *Trps1* deficient mice would reveal dental phenotypes characteristic for TRPS. This, in turn, would allow us to use these mice as a model to understand molecular and cellular abnormalities that lead to dental pathologies in this genetic disorder. The goal of this study was to identify morphological and mineralization defects in *Trps1* deficient mice, and the underlying molecular mechanisms.

2. Materials and Methods

2.1 Mice

All animal experiments complied with the National Institutes of Health guide for the care and use of laboratory animals, and were approved by the University of Alabama at Birmingham Institutional Animal Care and Use Committee. Generation and genotyping of *Trps1*$^{-/-}$ mice was described before [13,14]. Mice were maintained on mixed 129svev/C57B6 background. WT and *Trps1*$^{-/-}$ embryos were harvested at days 16.5 and 18.5 of gestation (E16.5 and E18.5, respectively). For tooth shape, size and mineral density analysis, specimens were collected from 4wk old WT and *Trps1*$^{+/-}$ male and female mice.

2.2 Microcomputed Tomography (μCT) Analyses

For the densitometric and volumetric analysis of dental tissues, hemimandibles of 4wk old mice (N=5/genotype/sex) were imaged in 70% ethanol by the Scanco μCT40 system (Scanco Medical AG, Brüttisellen, Switzerland) with a 10.5μm nominal resolution, 70kVp beam energy (at 145μA) and 200ms integration time. 3D reconstructed volumes were automatically generated by the system's software, which also performs automatic mineral density calibration for the scans' settings based on an algorithm. Analysis of enamel, crown dentin, and root mineralized tissues (dentin and cementum, together) were performed as described earlier [19] using histograms of mineral density and corresponding voxels within user-defined regions of interest around the anatomical crowns and roots of molars. Tissues of interest were segmented using global thresholds of 0.7 and 1.7g/cc mineral density values for segmentation of dentinal tissue from the pulpal cavity background and enamel from dentinal tissue, respectively. Mineral densities were expressed as weighted averages for the enamel, crown dentin, and root dentin and cementum voxels in respective distributions on the histograms and volumes for the same tissues were calculated from the respective areas under the curve.

2.3 Histology and Histomorphometric Analyses of Tooth Organs

Heads of E16.5 and E18.5 embryos were fixed in 4% paraformaldehyde for 24h, dehydrated and embedded in paraffin. Serial 7μm-thick sections were processed for standard H&E staining. The size of first mandibular molar tooth organs (N=3 embryos/genotype) was compared by measuring the anterior-posterior (AP) diameter and the height of mesial and distal buccal cusps (MBC and DBC, respectively) from the base of each tooth organ to the top of each cusp on H&E-stained sagittal sections. Measurements were performed under Zeiss Axioskop A1 microscope using Zeiss AxioVision software. Three consecutive sections were measured in each organ and the mean value was used for statistical analyses.

2.4 Immunohistochemistry (IHC)

IHC was performed using heat-induced antigen retrieval in sodium citrate buffer (pH 6.0) and primary antibodies: Runx2 (Santa Cruz, 1:600 dilution), Osx (Abcam, 1:200 dilution). Subsequently, sections were incubated with AlexaFluor 594-conjugated secondary antibody (Life Technologies) and ProLong Gold with DAPI Antifade Mountant (Molecular Probes, Thermo Fisher Scientific), and imaged using Nikon Eclipse 90i microscope. Percentage of

Runx2- and Osx-positive cells in cusp area of dental pulp was counted using NIS Elements software (N=3 mice/genotype). IHC detection of osteopontin (OPN) and osteocalcin (OC) was done in 7μm frozen serial sections using anti-osteopontin (Abcam, 1:100 dilution) and antiosteocalcin primary antibodies (Abcam, 1:200 dilution); goat anti-rabbit IgG H&L (HRP) secondary antibody (Abcam, 1:2000); and DAB Peroxidase (HRP) Substrate Kit (Vector Laboratories).

2.5 Cell Proliferation Analysis

Pregnant mice were injected intraperitoneally with 100mg/kg of body weight of 5-bromo-2'-deoxyuridine (BrdU; Sigma-Aldrich), 2h before euthanasia. Heads of E16.5 mice were fixed in 4% paraformaldehyde for 24h, and embedded in paraffin. 6μm sections were pretreated in 2N HCl for 1h, then incubated with anti-BrdU antibody (Abcam, 1:200 dilution) for 24h at 4°C, and counterstained with DAPI. Images were taken using Nikon Eclipse 90i microscope. BrdU positive signals were counted using NIS Elements software for N=3 mice/genotype.

2.6 Statistical Analysis

Histomorphometric and cell count analyses were done for N=3 mice/genotype; μCT analyses were done for N=5 mice/genotype. Values were expressed as mean ± standard deviation (SD). Statistical significant differences were determined using two-tailed t-test. Calculations were performed using GraphPad prism software. A *p*-value of ≤0.05 was considered statistically significant.

3. Results

3.1 Differential effect of the *Trps1* haploinsufficiency on the tooth size of male and female mice

Teeth of *Trps1*$^{+/-}$ mice are macroscopically indistinguishable from WT littermates. To evaluate dental phenotypes with a high sensitivity, teeth of 4wk old *Trps1*$^{+/-}$ and WT mice (male and female mice, separately) were compared using μCT. 3D renderings of μCT images revealed no differences in the tooth number (Fig.1A). Detailed comparisons of the crown shape of the first mandibular molars detected no morphological differences between *Trps1*$^{+/-}$ and WT teeth either (Fig.1B). However, volumetric μCT analyses revealed significantly decreased crown and root volumes of molars of *Trps1*$^{+/-}$ female mice in comparison with WT littermates ($p \leq 0.05$ and $p \leq 0.0005$, respectively; Fig. 1C). No difference in tooth size was detected between *Trps1*$^{+/-}$ and WT male mice, suggesting a sex-specific effect of Trps1 on the molar size in mice.

3.2 *Trps1* haploinsufficiency results in decreased mineralization of dental tissues

To investigate the effect of *Trps1* haploinsufficiency on mineralization of dental tissues, densitometric μCT analyses of first mandibular molars of 4wk old mice were performed (Fig.2). These analyses detected significantly reduced enamel mineral density in *Trps1*$^{+/-}$ male mice in comparison with WT males ($p \leq 0.05$), but no respective difference in female mice. Dentin mineral density was significantly reduced in both male and female *Trps1*$^{+/-}$ mice in comparison with WT littermates ($p \leq 0.005$). In the root, the dentin was analyzed together with cementum, since these two tissues cannot be distinguished from each other in

μCT images. Densitometric analyses of root mineralized tissues detected significantly reduced mineral density in *Trps1*$^{+/-}$ female mice in comparison with WT ($p \leq 0.005$), while no difference was detected between *Trps1*$^{+/-}$ and WT male mice (Fig.2). These results indicate that Trps1 is a regulator of mineralization of dental tissues in both the crown and the root.

3.3 Differences in expression of osteocalcin and osteopontin between WT and *Trps1*$^{+/-}$ mice.

Following the observation that tooth mineralization is decreased in *Trps1*$^{+/-}$ mice and results of published in vitro studies showing that Trps1 directly represses the osteocalcin (OC) gene [20], we compared expression of this mineralization-related protein in odontoblasts and dentin of WT and *Trps1*$^{+/-}$ male and female mice. In addition to understand better the molecular determinants of the detected differences in mineralization, we analyzed expression of another mineralization-related matrix protein osteopontin (OPN). Immunohistochemical analysis of OC and osteopontin OPN in WT and *Trps1*$^{+/-}$ first mandibular molars of 4 wk old male and female mice detected OC and OPN in both crown and root odontoblasts and dentin of WT mice (Fig. 3). In *Trps1*$^{+/-}$ females, decreased expression of OC and OPN proteins was detected in both crown and root odontoblasts and predentin in comparison with WT females (Fig. 3). However in males, changes in OC and OPN were detected only in the crown region, while in the root, no apparent differences were observed (Fig. 3A, B). Similarly to females, expression of OPN was decreased in *Trps1*$^{+/-}$ males in comparison with WT (Fig. 3B). In contrast, OC signal was stronger in *Trps1*$^{+/-}$ males crown dentin in comparison with WT males (Fig.3A).

3.4 Altered spacial expression of key osteogenic transcription factors in tooth organs of *Trps1*$^{-/-}$ mice

Considering that OC and OPN are direct targets of Runx2 and Osx and because expression of these two major osteogenic transcription factors was reported to be significantly decreased in *Trps1* deficient odontoblast in vitro, expression of Runx2 and Osx was subsequently evaluated by IHC (Fig. 4). For these analyses, we switched to *Trps1*$^{-/-}$ mice and E18.5 tooth organs, because *Trps1* is highly expressed prior to cytodifferentiation of dental cells and because of the dose-effect of *Trps1* deficiency. In E18.5 WT molar organs, high Runx2 expression was detected in the dental follicle and ameloblasts (Fig.4A). In addition, some odontoblasts and cells at the periphery of the dental pulp were positive for Runx2 in WT mice. In contrast, in *Trps1*$^{-/-}$ tooth organs, many of dental pulp cells, located at the periphery as well as inside the pulp, were positive for Runx2. In the cusp area specifically, there was an evident increase in the number of cells positive for Runx2. Quantitative analyses of the pulp cells in the cusp area confirmed this observation and demonstrated significantly increased number of Runx2-positive cells in *Trps1*$^{-/-}$ molar organs in comparison with WT ($p \leq 0.005$; Fig.4B).

Similarly, IHC analyses of Osx revealed expansion of Osx-positive cells in the cusp area of the *Trps1*$^{-/-}$ dental pulp in comparison with WT tooth organs, which was confirmed by quantitative analyses ($p \leq 0.05$; Fig.4C, D). However, unlike Runx2, which was expressed in the dental follicle and ameloblasts of both WT and *Trps1*$^{-/-}$ tooth organs, Osx was detected

in dental follicle and ameloblasts only in WT mice. In the dental follicle and ameloblasts of *Trps1*$^{-/-}$ mice, the expression of Osx was largely diminished (Fig.4C). In summary, the IHC results demonstrated that, at the cytodifferentiation stage of developing teeth, Trps1 regulates expression of major osteogenic transcription factors in a cell-type specific manner.

3.5 Trps1 deficiency results in smaller tooth organs

Differences in shape and size of WT and *Trps1*$^{-/-}$ first mandibular molar organs were noticed through the IHC analyses. To evaluate morphologic differences between WT and *Trps1*$^{-/-}$ tooth organs, histomorphometric analyses were utilized. The heights of the mesial buccal and distal buccal cusps, as well as the anterior-posterior diameter of WT and *Trps1*$^{-/-}$ first mandibular molar organs were measured in order to compare the overall tooth organ size (Fig.5A, B). These measurements showed significantly shorter anterior-posterior length of *Trps1*$^{-/-}$ tooth organs in comparison with WT mice ($p \leq 0.0005$; Fig.5C). The height of distal buccal cusp in *Trps1*$^{-/-}$ tooth organs showed a trend towards reduced height, which however did not reach the statistical significance ($p=0.057$). There was no difference in the height of the mesial buccal cusp of *Trps1*$^{-/-}$ and WT tooth organs (Fig.5C). From these results of histomorphometric analyses, we concluded that *Trps1* deficiency results in the decreased size of the first mandibular molar tooth organ.

3.6 Trps1 supports cell proliferation in dental mesenchyme and epithelium

To determine the underlying mechanisms of smaller *Trps1*$^{-/-}$ tooth organs, we next analyzed cell proliferation in developing *Trps1*$^{-/-}$ and WT tooth organs using BrdU incorporation assay. BrdU labeling of E16.5 mice detected significantly reduced number of proliferating cells in *Trps1*$^{-/-}$ tooth organs in comparison with WT (Fig.6). An approximately 50% decrease in the percentage of the BrdU-positive cells was detected in *Trps1*$^{-/-}$ tooth organs in comparison with WT ($p \leq 0.05$) in the dental mesenchyme. In the dental epithelium, *Trps1*$^{-/-}$ tooth organs had approximately 30% less of BrdU-positive cells than WT tooth organs ($p \leq 0.05$). These results indicate that *Trps1* is an important positive regulator of cell proliferation in both mesenchyme and epithelium of developing teeth.

4. Discussion

In this study, we used *Trps1*$^{+/-}$ and *Trps1*$^{-/-}$ mice to analyze the function of *Trps1* in tooth development, with the focus on aspects of tooth formation that are disturbed in TRPS. 4wk old *Trps1*$^{+/-}$ female and male mice were used to characterize dental phenotypes in fully developed teeth, and *Trps1*$^{-/-}$ embryos were used to determine molecular functions of *Trps1* during tooth development. Our analyses determined that disruption of one *Trps1* allele is sufficient to impair mineralization of dental tissues, which was associated with aberrant expression of mineralization-related matrix proteins OC and OPN, and to affect the size of teeth. Some of the differences between *Trps1*$^{+/-}$ and WT mice were sex-specific. Analyses of *Trps1*$^{-/-}$ embryos revealed that *Trps1* is a positive regulator of proliferation of both mesenchymal and epithelial cells in tooth organs. Furthermore, we show that *Trps1* regulates expression of major osteogenic transcription factors, in a cell type-specific manner.

Dental abnormalities are considered a characteristic feature of TRPS, although there is a significant variability of dental presentations even within families [5,7,11,21-25]. However, there is no systematic study of dental defects in TRPS patients and evaluations of dental phenotypes are frequently missing in clinical reports of TRPS. Hence, there is limited data available on the occurrence rate of dental manifestations. The comprehensive study by Maas et al. gathered information on 103 individuals with TRPS and attention was drawn to dental overcrowding which was commonly reported (68%)[5]. The authors also described that individuals with TRPS showed delayed eruption of the primary dentition, as well as microdontia.

Trps1$^{+/-}$ mice, similarly to TRPS patients, demonstrate microdontia, which was revealed by μCT analyses of postnatal molars and confirmed by histomorphometric analyses of *Trps1*$^{-/-}$ embryonic tooth organs (Fig.1 and 5). This shows that the function of *Trps1* in determining the size of a tooth is conserved between mice and humans. The decreased tooth size in *Trps1* deficient mice can be attributed to a developmental defect, specifically, to the significantly decreased proliferation of cells in developing tooth organs. The role of *Trps1* in cell proliferation has been demonstrated previously in developing endochondral bones and hair follicles [14,15,26], which are also affected in TRPS, demonstrating that this function of *Trps1* is cell type independent. Interestingly, although *Trps1* is highly expressed in dental mesenchyme [7], we detected decreased proliferation of both mesenchymal and epithelial cells in *Trps1*$^{-/-}$ mice (Fig.6). This suggests both cell autonomous and non-autonomous mechanism, by which Trps1 acts as a positive regulator of cell proliferation in developing tooth organs.

Similarly, the abnormal pattern of spatial expression of Runx2 and Osx detected in *Trps1*$^{-/-}$ tooth organs suggests a combination of cell autonomous and non-autonomous mechanisms, by which *Trps1* regulates expression of these two key osteogenic transcription factors. In *Trps1*$^{-/-}$ tooth organs, expression of both transcription factors expanded from the periphery of the dental pulp to cells located further away from it (Fig. 4). Considering that both Runx2 and Osx are highly expressed in dental mesenchyme and their expression becomes more restricted as tooth development progresses through the cytodifferentiation [27-29], their expanded expression in the *Trps1*$^{-/-}$ pulp may be indicative of delayed tooth development. Alternatively, the expanded expression of Runx2 may be a consequence of the loss of the repression of its gene. This possibility is supported by previous studies, which demonstrated expanded expression of *Runx2* in endochondral bones of *Trps1*$^{-/-}$ embryos and showed that *Runx2* promoter is directly repressed by the Trps1 transcription factor [14] In such a case, expanded Osx expression would be a consequence of the expanded Runx2 expression, as the Runx2 transcription factor regulates *Osx* expression. Interestingly, we detected that *Trps1*$^{-/-}$ ameloblasts and dental follicle cells are negative for Osx protein, which suggests that *Trps1* is required for Osx expression in these cells. However the mechanisms by which Trps1 activates the *Osx* gene in dental follicle are likely different from those in ameloblasts, since Trps1 is highly expressed in follicle, while its expression has not been detected in ameloblasts [7]. This suggests that Trps1 may directly activate *Osx* expression in dental follicle cell, while the Trps1-dependent activation of *Osx* in ameloblasts occurs though cell non-autonomous mechanisms, likely through involvement of signaling molecules [14,30].

Consistently with the previous report addressing supernumerarity in *Trps1*$^{-/-}$ mice[7], we did not detect tooth number aberration in analyzed mice, further supporting previous observation that this dental phenotype of TRPS is not reproduced in a mouse model of this disorder. This finding is not surprising, as molecular mechanisms regulating tooth number are different between mice and humans [31], and consequently mouse models of genetic disorders with supernumerary teeth often do not reproduce this abnormality [32]. However, considering that the supernumerarity is rare TRPS patients, it is plausible that, in some rare cases, this abnormality might occur in mice, as well.

Our study is the first one addressing mineralization of dental tissues in *Trps1* deficiency, although increased susceptibility to dental caries, which may be caused by defective mineralization of dental tissues, is frequent in TRPS patients. We uncovered that *Trps1* haploinsufficiency results in significantly decreased dentin mineral density. The requirement of Trps1 for dentin mineralization has been suggested by our previous *in vitro* studies with a preodontoblast cell line [18]. In this study, we have confirmed *in vivo* that *Trps1* plays a role in physiologic dentin mineralization. The mineral density of enamel and root tissues showed a trend towards decreased mineralization in *Trps1*$^{+/-}$ mice, although it was statistically significant only for enamel in male and for root tissues in female mice. The decreased mineral density of dental tissues may contribute to the high susceptibility to caries, which is one of the characteristic dental phenotypes in TRPS [5,6,10,11]. On the molecular level, this phenotype may result from dysregulated transcription, as Trps1, Runx2 and Osx are expressed in the same cell types during tooth development, and they regulate expression of genes involved in the mineralization process. For example, OC gene is directly regulated by Runx2, Osx and Trps1. We detected increased expression of OC in odontoblasts and predentin of *Trps1*$^{+/-}$ mice, which is consistent with previous in vitro studies showing that Trps1 represses the OC gene[20]. However the observed changes in OC and OPN do not faithfully mirror the mineralization defects detected in *Trps1*$^{+/-}$ mice. One possible reason for this discrepancy is a candidate approach, which we took to identify mineralization-related proteins affected by Trps1 deficiency. The limitation of a candidate approach is that it may miss other, more significant contributors to the phenotype. Global, unbiased approach of gene expression changes in Trps1-deficient odontoblasts would address this issue in a comprehensive way.

Interestingly, we detected that tooth size, aberrant expression of mineralization-related matrix proteins and mineralization defects are sex-specific in *Trps1*$^{+/-}$ mice. The sex-specific effect on mineralization is consistent with the report showing that *Trps1* differentially modulates bone mineral density between male and female mice and with the identification of a SNP in the *TRPS1* gene, which is differentially associated with bone mineral density in men and women [33]. Sex-specific differences in TRPS patients have been described with respect to hair and craniofacial abnormalities [3,5]. To the best of our knowledge, the only dental abnormality that has been detected more frequently in women than men is the congenital absence of teeth [6]. One of potential mechanisms underlying this may be an effect of sex hormones, as *Trps1* expression has been shown to be regulated by androgen and estrogen [34,35]. Of note, lower expression of mineralization-related genes in *Trps1*$^{+/-}$ mice does not completely correspond to the.

In conclusion, this study has shown that *Trps1* is involved in development of the tooth organ and formation of dental mineralized tissues. The role of *Trps1* in tooth size and mineralization is conserved between mice and human, hence $Trps1^{-/-}$ and $Trps1^{+/-}$ mice can be used as a model to uncover molecular abnormalities underlying dental pathologies in TRPS and to test therapeutic approaches for this disorder. The detection of sex-specific differences of *Trps1* haploinsufficiency on the formation of the tooth provides the base for in depth mechanistic studies of sex-specific determinants of mineralization of dental tissues and the mechanism of the interplay between Trps1 and these factors.

Acknowledgements

We would like to thank Ms. Rong Chong (School of Dental Medicine University of Pittsburgh) for assisting with μCT imaging and analyses. Research reported in this publication was supported by National Institute of Dental and Craniofacial Research of the National Institutes of Health under award number R01DE023083 (to D.N.) and by the Center for Craniofacial Regeneration, School of Dental Medicine University of Pittsburgh. The authors have no conflict of interest to declare.

7. References

1. Malik TH, Shoichet SA, Latham P, Kroll TG, Peters LL, Shivdasani RA. Transcriptional repression and developmental functions of the atypical vertebrate GATA protein TRPS1. The EMBO journal. 2001;20(7):1715–25. Epub 2001/04/04. doi: 10.1093/emboj/20.7.1715. PubMed PMID: 11285235; PMCID: PMC145487. [PubMed: 11285235]
2. Chang GT, van den Bemd GJ, Jhamai M, Brinkmann AO. Structure and function of GC79/TRPS1, a novel androgen-repressible apoptosis gene. Apoptosis : an international journal on programmed cell death. 2002;7(1): 13–21. Epub 2002/01/05. PubMed PMID: 11773701. [PubMed: 11773701]
3. Ludecke HJ, Schaper J, Meinecke P, Momeni P, Gross S, von Holtum D, Hirche H, Abramowicz MJ, Albrecht B, Apacik C, Christen HJ, Claussen U, Devriendt K, Fastnacht E, Forderer A, Friedrich U, Goodship TH, Greiwe M, Hamm H, Hennekam RC, Hinkel GK, Hoeltzenbein M, Kayserili H, Majewski F, Mathieu M, McLeod R, Midro AT, Moog U, Nagai T, Niikawa N, Orstavik KH, Plochl E, Seitz C, Schmidtke J, Tranebjaerg L, Tsukahara M, Wittwer B, Zabel B, Gillessen-Kaesbach G, Horsthemke B. Genotypic and phenotypic spectrum in tricho-rhino-phalangeal syndrome types I and III. American journal of human genetics. 2001;68(1):81–91. Epub 2000/12/12. PubMed PMID: 11112658; PMCID: PMC1234936. [PubMed: 11112658]
4. Momeni P, Glockner G, Schmidt O, von Holtum D, Albrecht B, Gillessen-Kaesbach G, Hennekam R, Meinecke P, Zabel B, Rosenthal A, Horsthemke B, Ludecke HJ. Mutations in a new gene, encoding a zinc-finger protein, cause tricho-rhino-phalangeal syndrome type I. Nature genetics. 2000;24(1):71–4. Epub 1999/12/30. doi: 10.1038/71717. PubMed PMID: 10615131. [PubMed: 10615131]
5. Maas SM, Shaw AC, Bikker H, Ludecke HJ, van der Tuin K, Badura-Stronka M, Belligni E, Biamino E, Bonati MT, Carvalho DR, Cobben J, de Man SA, Den Hollander NS, Di Donato N, Garavelli L, Gronborg S, Herkert JC, Hoogeboom AJ, Jamsheer A, Latos-Bielenska A, Maat-Kievit A, Magnani C, Marcelis C, Mathijssen IB, Nielsen M, Otten E, Ousager LB, Pilch J, Plomp A, Poke G, Poluha A, Posmyk R, Rieubland C, Silengo M, Simon M, Steichen E, Stumpel C, Szakszon K, Polonkai E, van den Ende J, van der Steen A, van Essen T, van Haeringen A, van Hagen JM, Verheij JB, Mannens MM, Hennekam RC. Phenotype and genotype in 103 patients with tricho-rhino-phalangeal syndrome. European journal of medical genetics. 2015;58(5):279–92. Epub 2015/03/21. doi: 10.1016/j.ejmg.2015.03.002. PubMed PMID: 25792522. [PubMed: 25792522]
6. Bennett CG, Hill CJ, Frias JL. Facial and oral findings in trichorhinophalangeal syndrome type 1 (characteristics of TRPS 1). Pediatric dentistry. 1981;3(4):348–52. Epub 1981/12/01. PubMed PMID: 6952172. [PubMed: 6952172]
7. Kantaputra P, Miletich I, Ludecke HJ, Suzuki EY, Praphanphoj V, Shivdasani R, Wuelling M, Vortkamp A, Napierala D, Sharpe PT. Tricho-rhino-phalangeal syndrome with supernumerary teeth.

Journal of dental research. 2008;87(11):1027–31. Epub 2008/10/24. doi: 10.1177/154405910808701102. PubMed PMID: 18946009. [PubMed: 18946009]

8. Vaccaro M, Guarneri F, Barbuzza O, Gaeta M, Guarneri C. A familial case of trichorhinophalangeal syndrome type I. Pediatric dermatology. 2009;26(2):171–5. Epub 2009/05/08. doi: 10.1111/j.1525-1470.2009.00905.x. PubMed PMID: 19419465. [PubMed: 19419465]
9. Rossi A, Devirgiliis V, Panasiti V, Borroni RG, Carlesimo M, Gentile M, Cariola F, Calvieri S. Missense mutation in exon 7 of TRPS1 gene in an Italian family with a mild form of trichorhinophalangeal syndrome type I. The British journal of dermatology. 2007;157(5):1021–4. Epub 2007/09/15. doi: 10.1111/j.1365-2133.2007.08158.x. PubMed PMID: 17854380. [PubMed: 17854380]
10. Candamourty R, Venkatachalam S, Karthikeyan B, Babu MR. Trichorhinophalangeal syndrome type 1: A case report with literature review. Journal of natural science, biology, and medicine. 2012;3(2):209–11. Epub 2012/12/12. doi: 10.4103/0976-9668.101936. PubMed PMID: 23225991; PMCID: PMC3510923.
11. Howell CJ, Wynne-Davies R. The tricho-rhino-phalangeal syndrome. A report of 14 cases in 7 kindreds. The Journal of bone and joint surgery British volume. 1986;68(2):311–4. Epub 1986/03/01. PubMed PMID: 3958020. [PubMed: 3958020]
12. Dumic M, Ille J, Mikecin M, Cvitkovic M, Hitrec V, Potocki K. [Trichorhinophalangeal syndrome]. Lijecnicki vjesnik. 1993;115(5-6): 163–5. Epub 1993/05/01. PubMed PMID: 8302139. [PubMed: 8302139]
13. Malik TH, Von Stechow D, Bronson RT, Shivdasani RA. Deletion of the GATA domain of TRPS1 causes an absence of facial hair and provides new insights into the bone disorder in inherited tricho-rhino-phalangeal syndromes. Molecular and cellular biology. 2002;22(24):8592–600. Epub 2002/11/26. PubMed PMID: 12446778; PMCID: PMC139891. [PubMed: 12446778]
14. Napierala D, Sam K, Morello R, Zheng Q, Munivez E, Shivdasani RA, Lee B. Uncoupling of chondrocyte differentiation and perichondrial mineralization underlies the skeletal dysplasia in tricho-rhino-phalangeal syndrome. Human molecular genetics. 2008;17(14):2244–54. Epub 2008/04/22. doi: 10.1093/hmg/ddn125. PubMed PMID: 18424451; PMCID: PMC2710999. [PubMed: 18424451]
15. Suemoto H, Muragaki Y, Nishioka K, Sato M, Ooshima A, Itoh S, Hatamura I, Ozaki M, Braun A, Gustafsson E, Fassler R. Trps1 regulates proliferation and apoptosis of chondrocytes through Stat3 signaling. Developmental biology. 2007;312(2):572–81. Epub 2007/11/13. doi: 10.1016/j.ydbio.2007.10.001. PubMed PMID: 17997399. [PubMed: 17997399]
16. Wuelling M, Kaiser FJ, Buelens LA, Braunholz D, Shivdasani RA, Depping R, Vortkamp A. Trps1, a regulator of chondrocyte proliferation and differentiation, interacts with the activator form of Gli3. Developmental biology. 2009;328(1):40–53. Epub 2009/04/25. doi: 10.1016/j.ydbio.2009.01.012. PubMed PMID: 19389374. [PubMed: 19389374]
17. Napierala D, Sun Y, Maciejewska I, Bertin TK, Dawson B, D'Souza R, Qin C, Lee B. Transcriptional repression of the Dspp gene leads to dentinogenesis imperfecta phenotype in Col1a1-Trps1 transgenic mice. Journal of bone and mineral research : the official journal of the American Society for Bone and Mineral Research. 2012;27(8):1735–45. Epub 2012/04/18. doi: 10.1002/jbmr.1636. PubMed PMID: 22508542; PMCID: PMC3399940.
18. Kuzynski M, Goss M, Bottini M, Yadav MC, Mobley C, Winters T, Poliard A, Kellermann O, Lee B, Millan JL, Napierala D. Dual role of the Trps1 transcription factor in dentin mineralization. The Journal of biological chemistry. 2014;289(40):27481–93. Epub 2014/08/17. doi: 10.1074/jbc.M114.550129. PubMed PMID: 25128529; PMCID: PMC4183789. [PubMed: 25128529]
19. Boskey AL, Verdelis K, Spevak L, Lukashova L, Beniash E, Yang X, Cabral WA, Marini JC. Mineral and matrix changes in Brtl/+ teeth provide insights into mineralization mechanisms. BioMed research international. 2013;2013:295812. Epub 2013/06/27. doi: 10.1155/2013/295812. PubMed PMID: 23802117; PMCID: PMC3681234. [PubMed: 23802117]
20. Piscopo DM, Johansen EB, Derynck R. Identification of the GATA factor TRPS1 as a repressor of the osteocalcin promoter. The Journal of biological chemistry. 2009;284(46):31690–703. Epub 2009/09/18. doi: 10.1074/jbc.M109.052316. PubMed PMID: 19759027; PMCID: PMC2797240. [PubMed: 19759027]

21. Goodman RM, Trilling R, Hertz M, Horoszowski H, Merlob P, Reisner S. New clinical observations in the trichorhinophalangeal syndrome. J Craniofac Genet Dev Biol. 1981;1(1):15–29. Epub 1981/01/01. PubMed PMID: 7341639. [PubMed: 7341639]
22. Hussels IE. Trichorhinophalangeal syndrome in two sibs. Birth Defects Orig Artic Ser. 1971;7(7):301–3. Epub 1971/06/01. PubMed PMID: 5173236.
23. Machuca G, Martinez F, Machuca C, Bullon P. Craniofacial and oral manifestations of trichorhinophalangeal syndrome type I (Giedion's syndrome): a case report. Oral Surg Oral Med Oral Pathol Oral Radiol Endod. 1997;84(1):35–9. Epub 1997/07/01. PubMed PMID: 9247947. [PubMed: 9247947]
24. Morioka D, Hosaka Y. Aesthetic and plastic surgery for trichorhinophalangeal syndrome. Aesthetic Plast Surg. 2000;24(1):39–45. Epub 2000/04/01. PubMed PMID: 10742468. [PubMed: 10742468]
25. Pashayan HM, Solomon LM, Chan G. The tricho-rhino-phalangeal syndrome. Am J Dis Child. 1974;127(2):257–61. Epub 1974/02/01. PubMed PMID: 4810280. [PubMed: 4810280]
26. Fantauzzo KA, Kurban M, Levy B, Christiano AM. Trps1 and its target gene Sox9 regulate epithelial proliferation in the developing hair follicle and are associated with hypertrichosis. PLoS genetics. 2012;8(11):e1003002. Epub 2012/11/08. doi: 10.1371/journal.pgen.1003002. PubMed PMID: 23133399; PMCID: PMC3486859. [PubMed: 23133399]
27. Clarke JC, Bae JM, Adhami M, Rashid H, Chen H, Napierala D, Gutierrez SE, Sinha K, Crombrugghe B, Javed A. Specificity protein 7 is not essential for tooth morphogenesis. Connective tissue research. 2014;55 Suppl 1:88–91. Epub 2014/08/27. doi: 10.3109/03008207.2014.923874. PubMed PMID: 25158188; PMCID: PMC4269224. [PubMed: 25158188]
28. D'Souza RN, Aberg T, Gaikwad J, Cavender A, Owen M, Karsenty G, Thesleff I. Cbfa1 is required for epithelial-mesenchymal interactions regulating tooth development in mice. Development (Cambridge, England). 1999;126(13):2911–20. Epub 1999/06/08. PubMed PMID: 10357935.
29. Kim TH, Bae CH, Lee JC, Kim JE, Yang X, de Crombrugghe B, Cho ES. Osterix regulates tooth root formation in a site-specific manner. Journal of dental research. 2015;94(3):430–8. Epub 2015/01/09. doi: 10.1177/0022034514565647. PubMed PMID: 25568170; PMCID: PMC4814021. [PubMed: 25568170]
30. Fantauzzo KA, Christiano AM. Trps1 activates a network of secreted Wnt inhibitors and transcription factors crucial to vibrissa follicle morphogenesis. Development (Cambridge, England). 2012;139(1):203–14. Epub 2011/11/26. doi: 10.1242/dev.069971. PubMed PMID: 22115758; PMCID: PMC3231778.
31. Jarvinen E, Salazar-Ciudad I, Birchmeier W, Taketo MM, Jernvall J, Thesleff I. Continuous tooth generation in mouse is induced by activated epithelial Wnt/beta-catenin signaling. Proceedings of the National Academy of Sciences of the United States of America. 2006;103(49):18627–32. Epub 2006/11/24. doi: 10.1073/pnas.0607289103. PubMed PMID: 17121988; PMCID: PMC1693713. [PubMed: 17121988]
32. Aberg T, Cavender A, Gaikwad JS, Bronckers AL, Wang X, Waltimo-Siren J, Thesleff I, D'Souza RN. Phenotypic changes in dentition of Runx2 homozygote-null mutant mice. The journal of histochemistry and cytochemistry : official journal of the Histochemistry Society. 2004;52(1):131–9. Epub 2003/12/23. doi: 10.1177/002215540405200113. PubMed PMID: 14688224. [PubMed: 14688224]
33. Wang L, Lu W, Zhang L, Huang Y, Scheib R, Liu X, Myers L, Lu L, Farber CR, Liu G, Wang CY, Deng H, Williams RW, Wang Y, Gu W, Jiao Y. Trps1 differentially modulates the bone mineral density between male and female mice and its polymorphism associates with BMD differently between women and men. PloS one. 2014;9(1):e84485. Epub 2014/01/15. doi: 10.1371/journal.pone.0084485. PubMed PMID: 24416236; PMCID: PMC3885592. [PubMed: 24416236]
34. Chang GT, Jhamai M, van Weerden WM, Jenster G, Brinkmann AO. The TRPS1 transcription factor: androgenic regulation in prostate cancer and high expression in breast cancer. Endocrine-related cancer. 2004;11(4):815–22. Epub 2004/12/23. doi: 10.1677/erc.1.00853. PubMed PMID: 15613454. [PubMed: 15613454]
35. Chen JQ, Litton J, Xiao L, Zhang HZ, Warneke CL, Wu Y, Shen X, Wu S, Sahin A, Katz R, Bondy M, Hortobagyi G, Berinstein NL, Murray JL, Radvanyi L. Quantitative immunohistochemical analysis and prognostic significance of TRPS-1, a new GATA transcription factor family member,

in breast cancer. Hormones & cancer. 2010;1(1):21–33. Epub 2010/02/01. doi: 10.1007/s12672-010-0008-8. PubMed PMID: 21761348. [PubMed: 21761348]

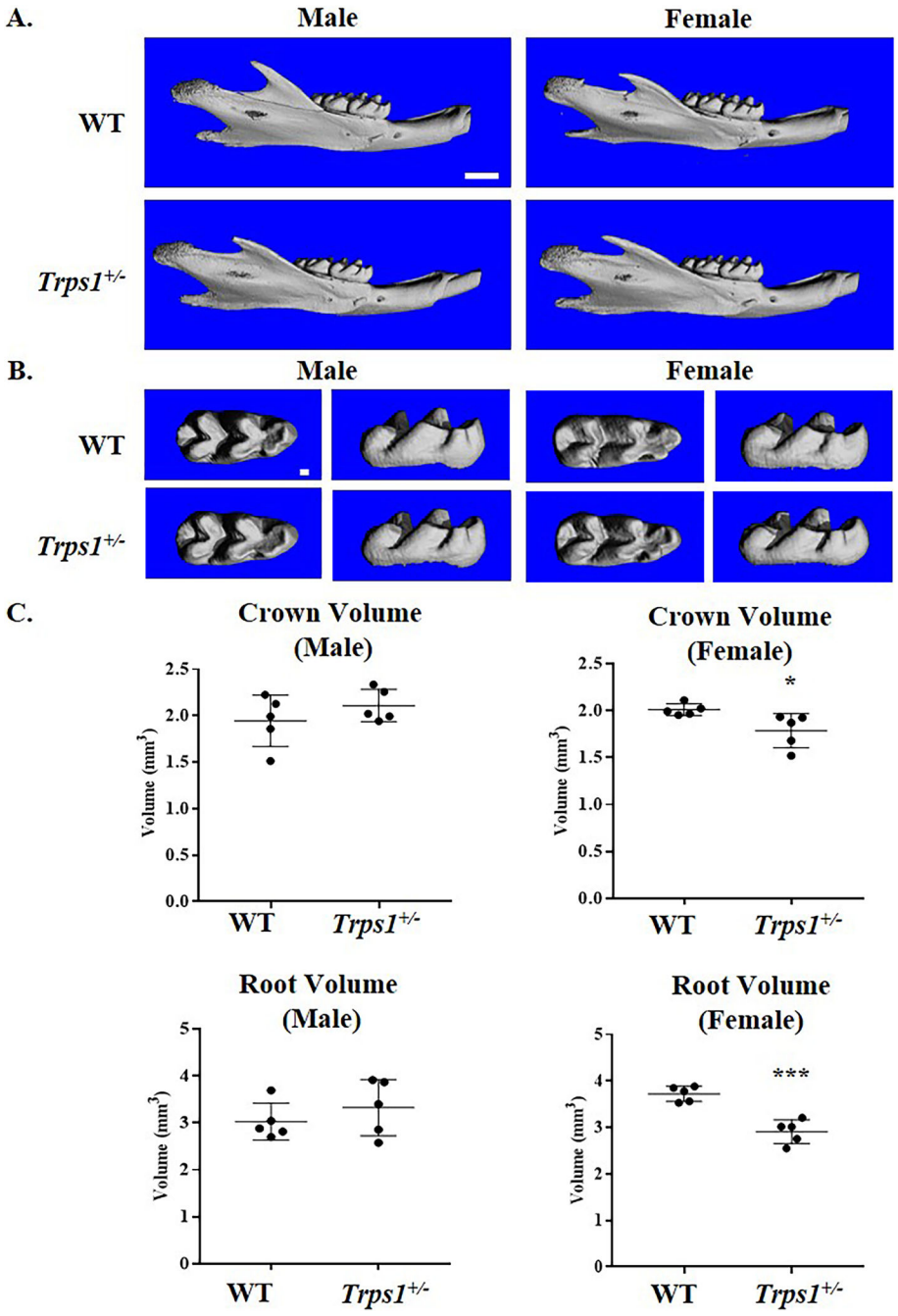

Figure 1. µCT analyses of tooth shape and size of 4wk old WT and *Trps1*$^{+/-}$ male and female mice.

(**A)** Representative images of 3D reconstruction of the mandible (lateral view), scale bar =1mm. (**B)** 3D reconstruction of first mandibular molars, scale bar =100µm. (**C)** Quantitative analysis of total crown volume and root volume of first mandibular molars. Graphs show individual values from each mouse, mean values ± SD (N=5 mice/genotype). *p≤0.05, ***p ≤0.0005.

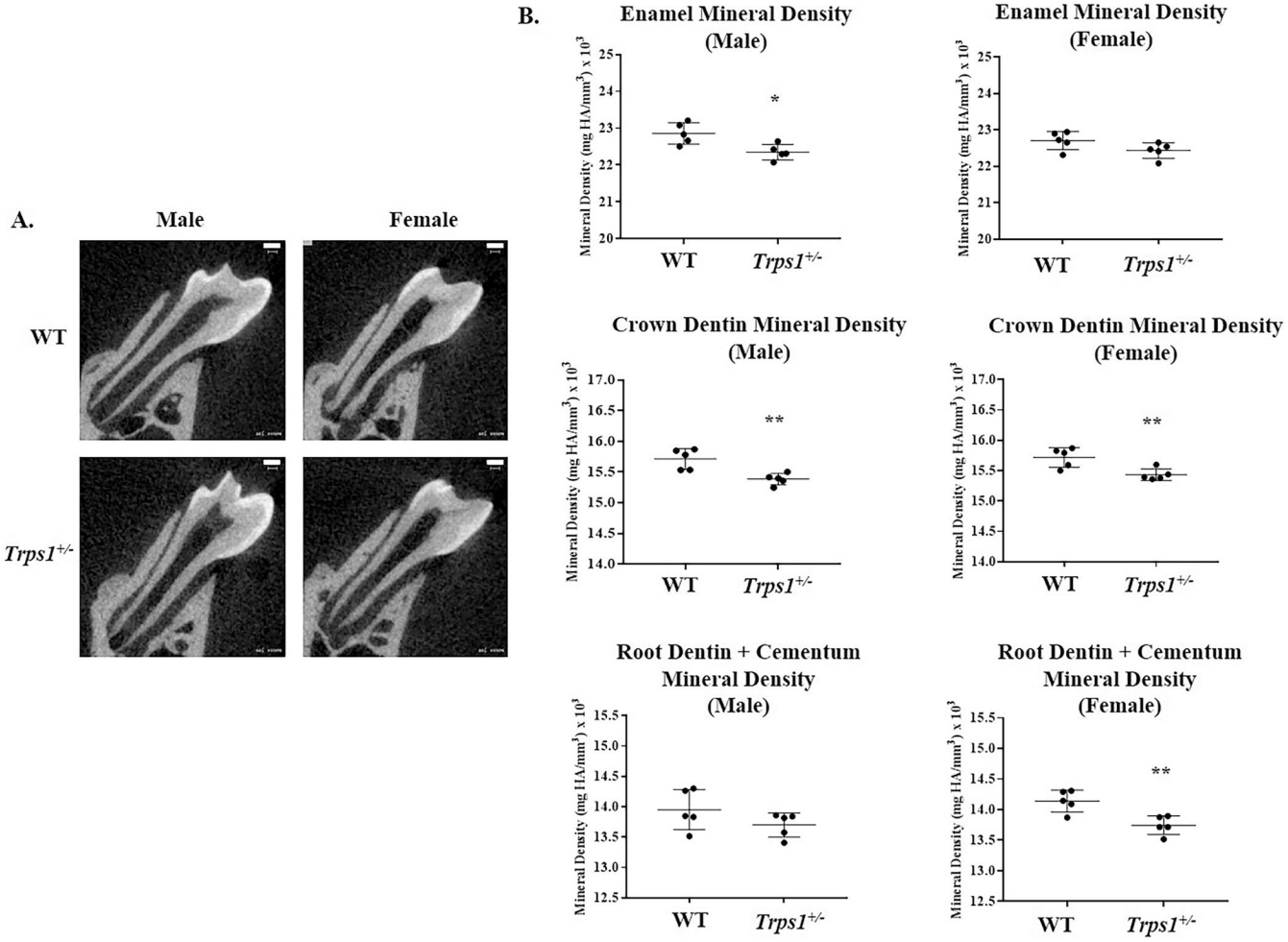

Figure 2. µCT analyses of mineral density of dental tissues of 4 wk old WT and *Trps1*$^{+/-}$ male and female mice.

(**A)** Representative two-dimensional images of first mandibular molars, scale bar =100µm. (**B)** Graphs showing quantitative analysis of enamel (upper panel), crown dentin (middle panel) and root (lower panel) mineral density of WT and *Trps1*$^{+/-}$ male and female mice (N=5 mice/genotype). Graphs show individual values from each mouse, mean values ± SD (N=5 mice/genotype). *p≤0.05, **p ≤0.005.

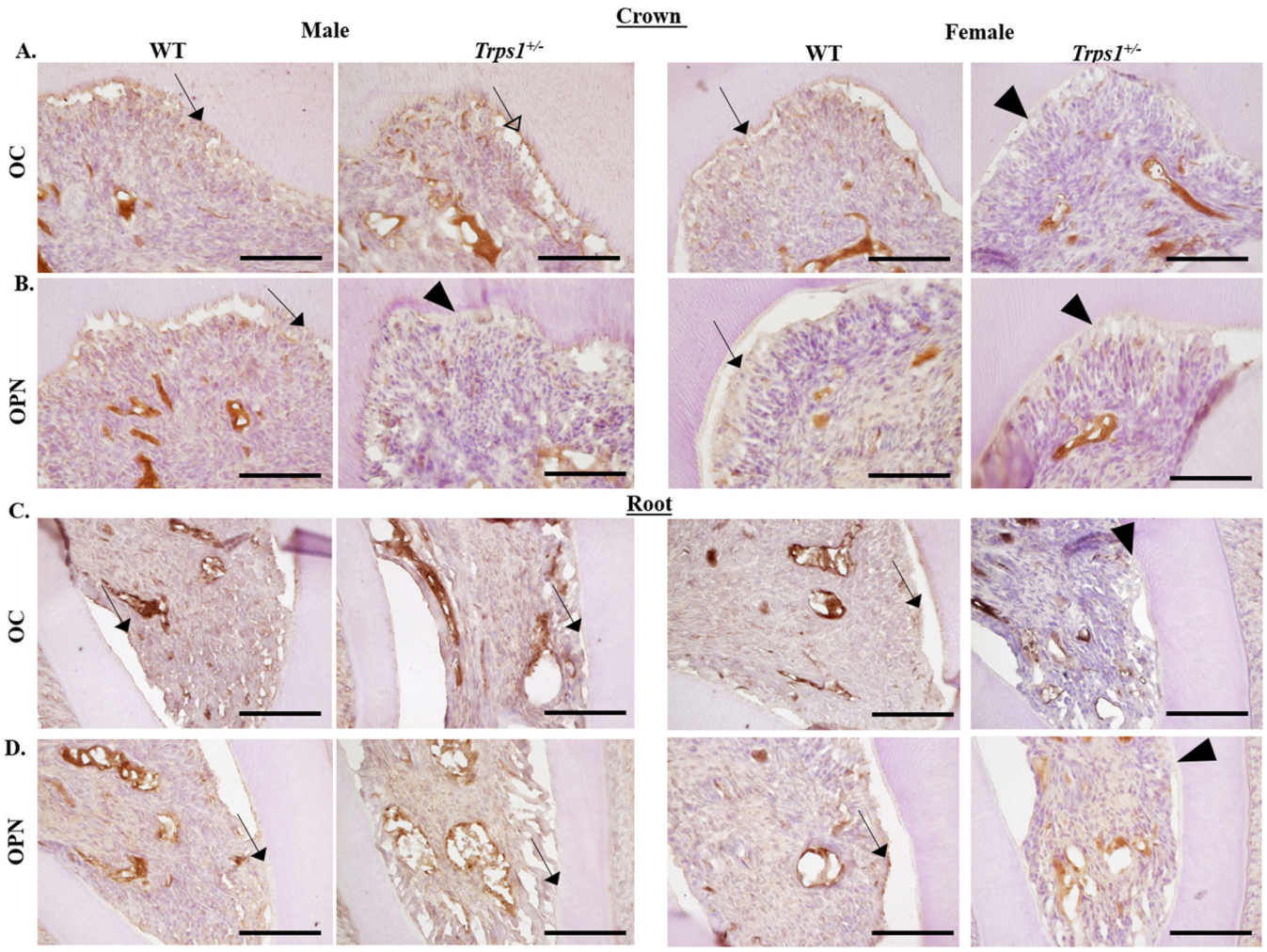

Figure 3. Immunohistochemical analysis of osteocalcin (OC) and osteopontin (OPN) in WT and *Trps1*$^{+/-}$ first mandibular molars of 4 wk old male and female mice.

(**A, B**) Representative images of sagittal sections of the crown portion of the molars. **(C, D)** Representative images of sagittal sections of the root portion of the molars. OC and OPN are detected in both crown and root odontoblasts and dentin of WT female and male mice (arrows). In *Trps1*$^{+/-}$ females, decreased expression of OC and OPN proteins was detected in both crown and root odontoblasts (arrowheads) in comparison with WT females. In *Trps1*$^{+/-}$ male mice, stronger OC signal was detected in crown odontoblasts and dentin (open arrowhead), while the expression of OPN was decreased (arrowhead) in comparison with WT males. Scale bars=100μm.

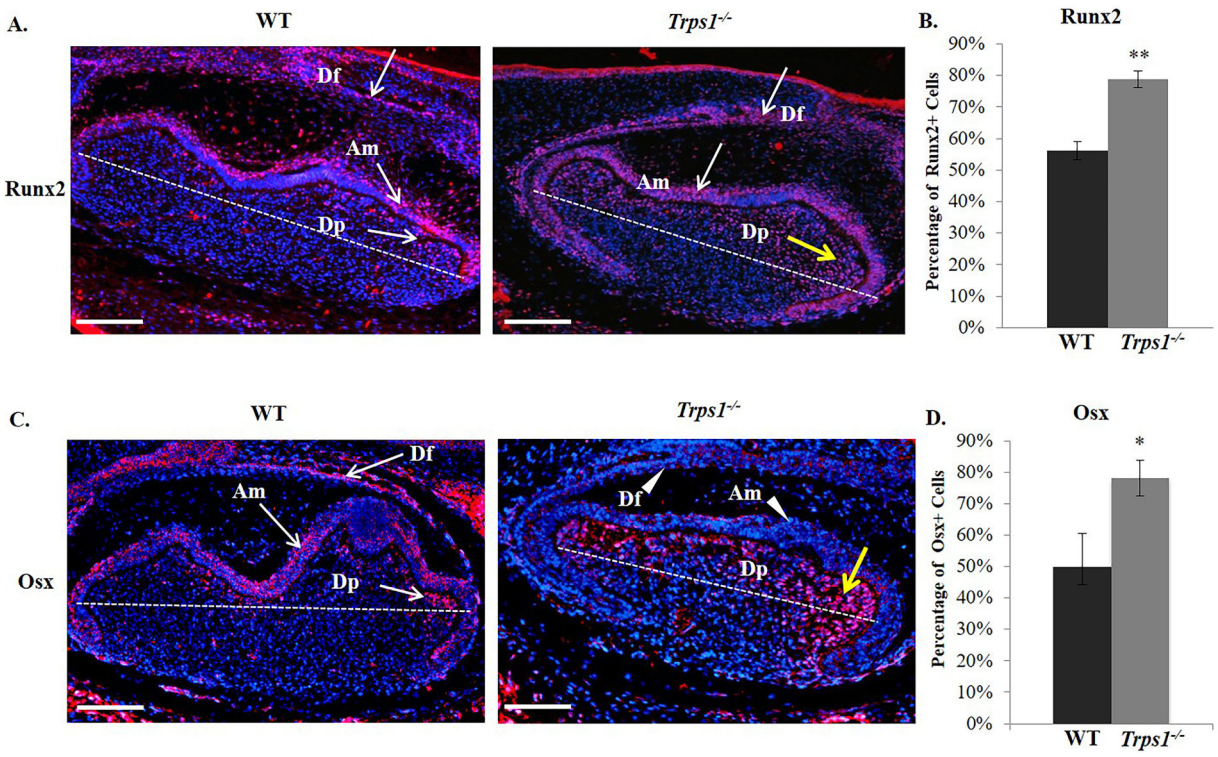

Figure 4. Differences in spatial distribution of Runx2 and Osx osteogenic transcription factors in first mandibular molar tooth organs of E18.5 WT and *Trps1*$^{-/-}$ mice.

(A) Representative images of sagittal sections of tooth organs stained with anti-Runx2 antibody (red). Runx2 (arrows) is detected in the dental follicle (Df) and ameloblasts (Am) in both WT and *Trps1*$^{-/-}$ mice. In the dental pulp (Dp), only some cells at the periphery are positive for Runx2 in WT mice, while in *Trps1*$^{-/-}$ mice, numerous Runx2-positive cells (yellow arrow) are detected within the pulp, in particular in the cusp area (above the dotted line). Images are shown in 10x magnification, scale bar =500px. **(B)** Quantification of the percentage of Runx2-positive cells (in the dental pulp region above the dotted line on the image on the left) in WT and *Trps1*$^{-/-}$ mice. Data are presented as mean values ± SD (N=3 mice/genotype). **p≤0.005. (**C**) Representative images of sagittal sections of tooth organs stained with anti-Osx antibody (red). In WT mice, Osx (arrows) is detected in the dental follicle (Df), ameloblasts (Am) and in cells at the periphery of the dental pulp (Dp). In *Trps1*$^{-/-}$ mice, Osx is detected only in the dental pulp cells (yellow arrow), while dental follicle cells and ameloblasts are negative for Osx (arrowheads). (**D**). Quantification of the percentage of Osx-positive cells in the dental pulp region above the dotted line on the image on the left) in WT and *Trps1*$^{-/-}$ mice. Data are presented as mean values ± SD (N=3 mice/genotype). *p≤0.05.

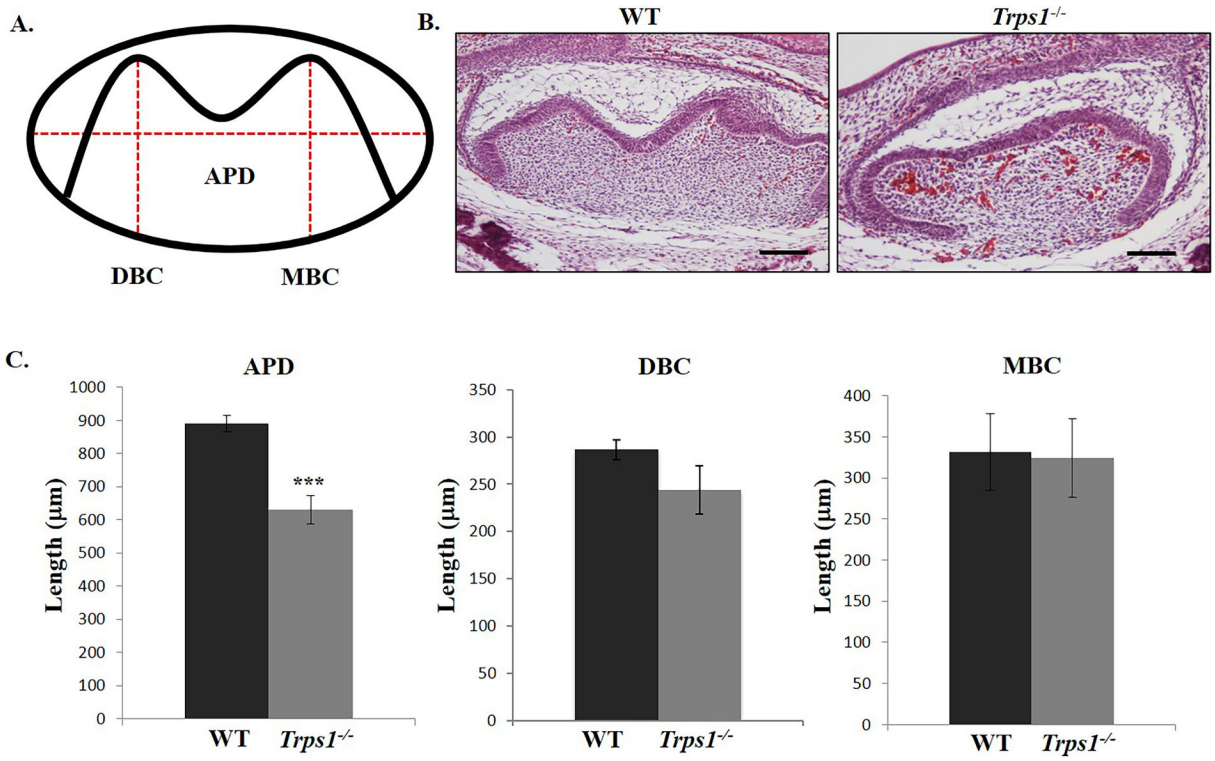

Figure 5. Comparison of the tooth organ dimensions (first mandibular molar) of E18.5 WT and *Trps1*$^{-/-}$ mice.

(A) Schematic of a tooth organ showing measurements of anterior-posterior diameter (APD), distal buccal cusp height (DBC) and mesial cusp height (MBC). **(B)** Representative images of H&E-stained sagittal sections at the midline of E18.5 tooth organs. Scale bar =250µm. (**C)** Graphs comparing APD, DBC height and MBC height of tooth organs of WT and *Trps1*$^{-/-}$ mice. Data are presented as mean values ± SD from equivalent sections (N=3 mice/genotype). ***p ≤0.0005.

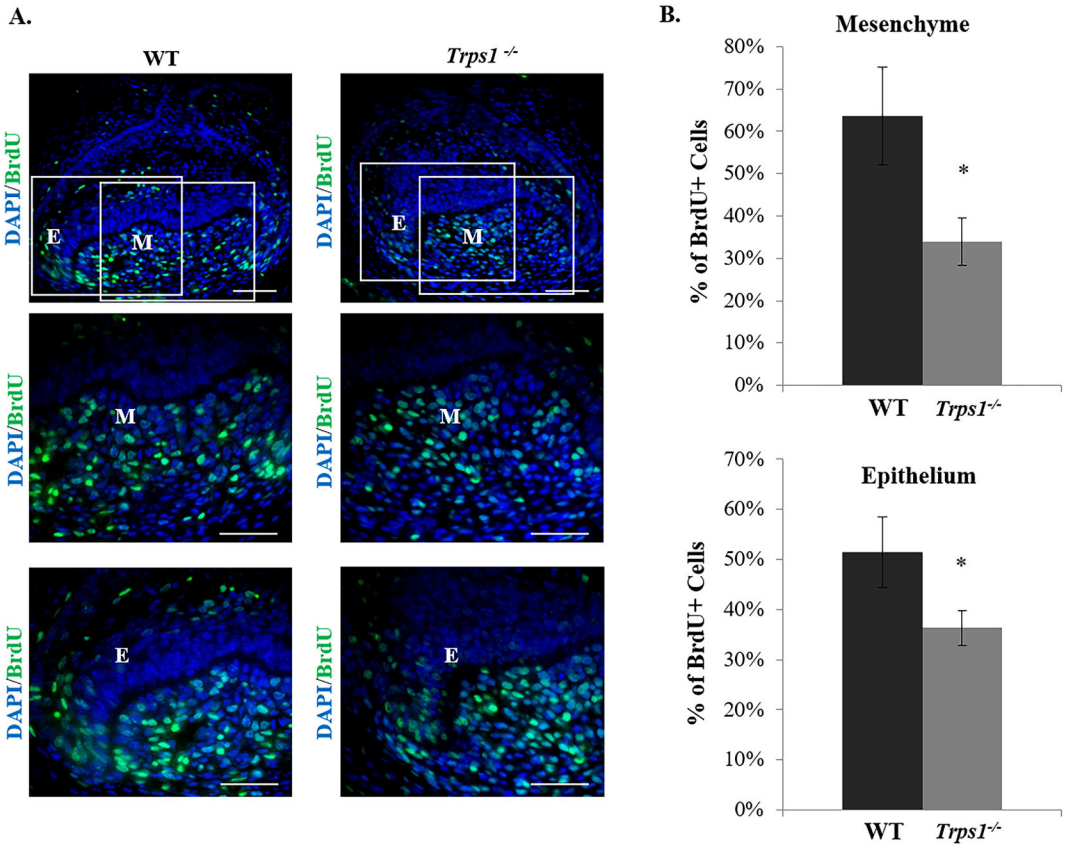

Figure 6. Analyses of cell proliferation in tooth organs of E16.5 WT and *Trps1*$^{-/-}$ mice.

(A) Representative images of IHC staining showing BrdU positive cells (green) in the first mandibular molar tooth organs of E16.5 mice. Boxed areas on the top panel images indicate areas within the dental epithelium (E) and dental mesenchyme (M), which are shown on the middle and bottom panels. Scale bar =50μm. (**B**) Graphs showing percentages of BrdU positive cells within the mesenchyme and epithelium of WT and *Trps1*$^{-/-}$ tooth organs. Data are presented as mean values ± SD (N=3 mice/genotype). *p≤0.05.